Rubnitz, J.E., Raimondi, S.C., Onciu, M., Coustan-Smith, E., Kun, L.E., Jeha, S., Cheng, C., Howard, S.C., Simmons, V., Bayles, A., Metzger, M.L., Boyett, J.M., Leung, W., Handgretinger, R., Downing, J.R., Evans, W.E. & Relling, M.V. (2009) Treating childhood acute lymphoblastic leukemia without cranial irradiation. *New England Journal of Medicine*, **360,** 2730–2741.

Pullen, J., Shuster, J.J., Link, M., Borowitz, M., Amylon, M., Carroll, A.J., Land, V., Look, A.T., McIntyre, B. & Camitta, B. (1999) Significance of commonly used prognostic factors differs for children with T cell acute lymphocytic leukemia (ALL), as compared to those with B-precursor ALL. A Pediatric Oncology Group (POG) study. *Leukemia*, **13,** 1696–1707.

Schneider, N.R., Carroll, A.J., Shuster, J.J., Pullen, D.J., Link, M.P., Borowitz, M.J., Camitta, B.M., Katz, J.A. & Amylon, M.D. (2000) New recurring cytogenetic abnormalities and association of blast cell karyotypes with prognosis in childhood T-cell acute lymphoblastic leukemia: a pediatric oncology group report of 343 cases. *Blood*, **96,** 2543–2549.

Schrauder, A., Reiter, A., Gadner, H., Niethammer, D., Klingebiel, T., Kremens, B., Peters, C., Ebell, W., Zimmermann, M., Niggli, F., Ludwig, W.D., Riehm, H., Welte, K. & Schrappe, M. (2006) Superiority of allogeneic hematopoietic stem-cell transplantation compared with chemotherapy alone in high-risk childhood T-cell acute lymphoblastic leukemia: results from ALL-BFM 90 and 95. *Journal of Clinical Oncology*, **24,** 5742–5749.

Weng, A.P., Ferrando, A.A., Lee, W., Morris, J.P. IV, Silverman, L.B., Sanchez-Irizarry, C., Blacklow, S.C., Look, A.T. & Aster, J.C. (2004) Activating mutations of NOTCH1 in human T cell acute lymphoblastic leukemia. *Science*, **306,** 269–271.

Winter, S.S., Jiang, Z., Khawaja, H.M., Griffin, T., Devidas, M., Asselin, B.L. & Larson, R.S. (2007) Identification of genomic classifiers that distinguish induction failure in T-lineage acute lymphoblastic leukemia: a report from the Children's Oncology Group. *Blood*, **110,** 1429–1438.

Zuurbier, L., Homminga, I., Calvert, V., te Winkel, M.L., Buijs-Gladdines, J.G., Kooi, C., Smits, W.K., Sonneveld, E., Veerman, A.J., Kamps, W.A., Horstmann, M., Petricoin, III, E.F., Pieters, R. & Meijerink, J.P. (2010) NOTCH1 and/or FBXW7 mutations predict for initial good prednisone response but not for improved outcome in pediatric T-cell acute lymphoblastic leukemia patients treated on DCOG or COALL protocols. *Leukemia*, **24,** 2014–2022.

Pediatric and Developmental Pathology 14, 87–92, 2011
DOI: 10.2350/08-12-0579.1

ORIGINAL ARTICLES

Neuroblastomas with Discordant Genotype-Phenotype Relationships: Report of Four Cases with *MYCN* Amplification and Favorable Histology

Atsuko Nakagawa,[1*] Kentaro Matsuoka,[1] Hajime Okita,[1] Hideto Iwafuchi,[2] Hisanari Hori,[3] and Masaaki Kumagai[4]

[1]Department of Pathology, National Center for Child Health and Development, Tokyo, Japan
[2]Department of Pathology, Aichi Medical University Hospital, Aichi, Japan
[3]Department of Pediatrics, Aichi Medical University Hospital, Aichi, Japan
[4]Department of Hematology, National Center for Child Health and Development, Tokyo, Japan

Received December 29, 2008; accepted December 10, 2009; published online December 14, 2009.

ABSTRACT

MYCN amplification prevents cellular differentiation and promotes mitotic and karyorrhectic activities in neuroblastomas. Hence, *MYCN*-amplified tumors typically show an appearance of neuroblastoma of either an undifferentiated or a poorly differentiated subtype with a high mitosis-karyorrhexis index. In addition, they are classified as part of the unfavorable histology group, according to the International Neuroblastoma Pathology Classification. Large cell type and/or presence of prominent nucleoli is also reported to be an additional hallmark of *MYCN* amplification. However, there are few neuroblastomas having *MYCN* amplification and favorable histology. Four cases of *MYCN* amplification and favorable histology were identified in our file of 63 cases of neuroblastoma. The patients (M:F = 3:1) were diagnosed between 6 and 13 months of age, and all had adrenal primary tumors and were treated with high-dose therapy and autologous stem cell rescue. Three patients (stages 1, 3, and 4) are alive and well 7 years, 26 months, and 19 months after diagnosis, respectively. One patient with stage 4 disease died 8 months after diagnosis. Their tumors showed the same histologic feature of neuroblastoma: poorly differentiated subtype with a low mitosis-karyorrhexis index; they were not qualified as large cell type and had no prominent nucleoli. *MYCN* amplification of those tumors was confirmed by fluorescence in situ hybridization in all 4 cases, but MYCN protein expression was not demonstrated by immunohistochemistry (4 cases) and *MYCN* mRNA was not detected by reverse transcriptase polymerase chain reaction (1 case). Those cases showed a discrepant genotype-phenotype that was not simply a laboratory observation but could indicate the concept that that *MYCN* amplification did not automatically equate to a poor prognosis in this group of patients.

Key words: favorable histology, *MYCN* amplification, neuroblastoma

INTRODUCTION

Peripheral neuroblastic tumors (PNTs) (including neuroblastoma, ganglioneuroblastoma, and ganglioneuroma) offer one of the best models for investigating biologically and clinically relevant relationships between their molecular/genetic alterations and morphologic manifestations. Reproducible correlation of *MYCN* gene amplification, an indicator for a poor prognosis, and specific histologic appearance in PNTs has been documented. *MYCN*-amplified tumor has no or limited potential of neuroblastic differentiation and is characterized by markedly increased mitotic and karyorrhectic activities. Therefore *MYCN*-amplified neuroblastoma is usually evaluated as either an undifferentiated or a poorly differentiated subtype with a high mitosis-karyorrhexis index (MKI) and unfavorable histology (UH), according to the International Neuroblastoma Pathology Classification (INPC) [1,2]. It is also reported that there is a significant association between *MYCN* amplification and specific cytologic features, such as large cell type and presence of

This work was supported by Grant-in-Aid for Scientific Research (A)(19209054).

*Corresponding author, e-mail: nakagawa-a@ncchd.go.jp

prominent nucleoli [3–6], also indicating aggressive behavior of PNTs. In contrast, favorable histology (FH) tumors are usually known to have a nonamplified *MYCN* gene.

There are, however, rare PNT cases presenting with a discordant genotype-phenotype relationship. In this report, we describe 4 cases whose tumors had amplified *MYCN* but were classified into the FH group and summarize those cases with the same genotype-phenotype discordance in literature.

MATERIALS AND METHODS

Four cases of neuroblastomas with *MYCN* amplification and FH (*MYCN*-A&FH) were identified among 63 cases of PNTs from the Department of Pathology, Aichi Medical University, and the National Center for Child Health and Development. The patients' clinical information was obtained from the medical records of each institution. The appropriate written informed consent was obtained from the parents. A presentation of the cases follows.

Case 1. This patient presented with an abdominal mass at the age of 6 months. Clinical study with computer tomography demonstrated a right suprarenal tumor. After complete resection of this stage 1 neuroblastoma, the patient received radiation therapy in the tumor bed and chemotherapy (vincristine and cyclophosphamide) for 6 months. Ten months after completion of the chemotherapy, she developed bone recurrence in the right 6th rib. Then she received reinduction/high-dose therapy (cyclophosphamide, vincristine, pirarubicin, cisplatin, etoposide/melphalan, etoposide, and carboplatin) and total body irradiation with autologous peripheral blood stem cell transplantation (PBSCT). The patient is alive and well 91 months after diagnosis.

Case 2. This patient presented with intra-abdominal bleeding due to the rupture of a right adrenal tumor at the age of 9 months. After incomplete resection of stage 3 neuroblastoma, the patient received induction/high-dose chemotherapy (cyclophosphamide, vincristine, pirarubicin, cisplatin/melphalan, etoposide, and carboplatin) with autologous PBSCT and radiation therapy. He has been followed with 13-*cis*-retinoic acid and is now alive and well 26 months after diagnosis.

Case 3. This patient presented with a right adrenal tumor and a nodular lesion of 3 cm in diameter in the right lung (stage 4) at the age of 13 months. After having the diagnosis of adrenal neuroblastoma by biopsy, the patient received induction/high-dose chemotherapy (cyclophosphamide, vincristine, pirarubicin, cisplatin/melphalan, etoposide, and carboplatin) with autologous PBSCT. However, he had tumor progression and died 8 months after diagnosis.

Case 4. This patient presented with an adrenal mass and bone marrow metastasis (stage 4) at the age of 13 months. After having biopsy diagnosis of neuroblastoma from both lesions, the patient was treated with induction/high-dose chemotherapy (cyclophosphamide, vincristine, pirarubicin, cisplatin/melphalan, etoposide, and carboplatin) and autologous PBSCT. He is alive and well 19 months after diagnosis.

Formalin-fixed, paraffin-embedded tumor specimens from the 4 patients were obtained at the time of diagnosis and before chemotherapy/irradiation therapy to determine the *MYCN* status and evaluate the histology/cytology. *MYCN* gene amplification was confirmed by dual-color fluorescence in situ hybridization using a Spectrum green-labeled chromosome 2p telomere probe (TelVysion 2p SpectrumGreen, Vysis, Downers Grove, IL, USA) and a Spectrum orange-labeled locus-specific *MYCN* probe (Vysis LSI N-MYC, Vysis) [7]. Histologic evaluation (determination of Schwannian stromal development, grade of neuroblastic differentiation, and MKI) was performed with hematoxylin and eosin–stained sections, according to the INPC [1,2], and cytologic evaluation (determination of large cell type or not and presence or absence of prominent nucleoli) was performed using the criteria reported by Tornoczky and colleagues [4].

MYCN protein expression was determined immunohistochemically using the same FFPE specimen from those 4 tumors with anti-MYCN protein mouse monoclonal antibody (ab-1, 1:400, oncogene, Cambridge, MA, USA), according to the standard avidin-biotin-peroxydase method. Antigen retrieval procedure was performed by autoclave heating at 121°C in citrate buffer (pH 7.0) for 7 minutes. For positive and negative controls, MYCN protein immunostaining was also performed on *MYCN* amplified and UH (*MYCN*-A&UH, 10 cases) tumors, *MYCN* nonamplified and UH (*MYCN*-nA&UH, 10 cases) tumors, and *MYCN* nonamplified and FH (*MYCN*-nA&FH, 10 cases) tumors. Negative control reaction was also obtained by deleting the primary antibody against MYCN protein.

In 1 case (case 1), snap-frozen tumor material was available for determining *MYCN* expression status at the mRNA level by reverse transcriptase polymerase chain reaction (RT-PCR). Total RNA was extracted from the tumor using RNeasy Mini kit (Qiagen, Tokyo, Japan) and treated with RNase free DNase I (Qiagen) according to manufacturer's instructions. The oligonucleotide primers for the human *MYCN* gene [sense: (5′) AGT TCC TTC CAC CCT CTC CT; antisense: (5′) CAC CCA GCA ACC CCC TAA AC], specific for a 151–base pair intronic sequence (intron 2), and the PCR conditions were described previously by Gilbert and colleagues [8].

RESULTS

Clinicopathologic characteristics of the 4 cases are summarized in Table 1. As shown in Figure 1, *MYCN* amplification in these tumors was confirmed by fluorescence in situ hybridization. It was noted that all tumors had the same histologic evaluation of neuroblastoma (Schwannian stroma poor): poorly differentiated subtype with a low MKI, according to the INPC (Fig. 2). No tumors had a cytologic appearance characteristic for large

Table 1. Summary of 4 neuroblastoma cases with amplified *MYCN* and favorable histology

Case	Age (months/sex)	Primary site	Clinical stage	Histology/cytology			MYCN protein	Follow up (months)
				Subtype	MKI	Large cell/prominent nucleoli		
1	6/female	Adrenal	1	Poorly diff.	Low	No/no	Negative	Alive (91)
2	9/male	Adrenal	3	Poorly diff.	Low	No/no	Negative[a]	Alive (26)
3	13/male	Adrenal	4	Poorly diff.	Low	No/no	Negative	Dead (8)
4	13/male	Adrenal	4	Poorly diff.	Low	No/no	Negative	Alive (19)

Age indicates months at diagnosis; follow up, months after diagnosis; clinical stage, according to the International Neuroblastoma Staging System; poorly diff., poorly differentiated neuroblastoma; MKI, mitosis-karyorrhexis index; large cell, large cell type neuroblastoma; MYCN protein, detected by immunohistochemistry.
[a]Few (<1%) tumor cells showed positive nuclear staining.

Table 2. MYCN-amplified and favorable histology neuroblastoma in the literature[a]

Age (months)	Stage	Histology (MKI)	Follow up (months)	Author
15	Localized	NBL, poorly diff.	Alive (66+)[b]	Cohn and colleagues [13]
16	Localized	NBL, poorly diff.	Alive (68+)[b]	
46	Localized	GNB	Alive (38)	
7	I	NBL	Alive (36)[c]	Goto and colleagues [14]
<12	III	NBL	Alive	
<12	IV	NBL	Alive	
<12	IV	NBL	Dead	
12~18	IV	NBL	Alive	
12~18	III	NBL	Dead	
12~18	IV	NBL	Dead	
12~18	IV	NBL	Dead	
0.1	IVS	NBL	Alive	Shimada and colleagues [15]
8.7	IV	NBL	Dead	
12.2	II	NBL	Alive (76)	
0.24	3	NBL, poorly diff. (low)	Alive (6)	George and colleagues [16]
2.4	3	NBL, poorly diff. (low)	Alive (8)	
3.6	3	NBL, poorly diff. (low)	Alive (17)	
15.6	2	NBL, poorly diff. (intermed.)	Alive (17)	
36	4	NBL, diff. (low)	Alive (6)	
43	I	GNB	Alive (17)	Fabbretti and colleagues [17]
48	II	GNB	Alive (16)	
9	2b	NBL	Dead (10)	Perez and colleagues [18]
7	1	NBL	Alive (17)	
0.16	1	NBL	Alive (72)	
4	A	NBL	Alive (53+)	Alvarado and colleagues [19]
4	A	NBL	Alive (59+)	
8	A	NBL	Alive (36+)	

Age indicates months at diagnosis; follow up, months after diagnosis; stage, I–IV and IVS, according to Evans' clinical staging; 2–4, according to the International Neuroblastoma Staging System; A, according to the Pediatric Oncology Group grading system; MKI, mitosis-karyorrhexis index; NBL, neuroblastoma; GNB, ganglioneuroblastoma; poorly diff., poorly differentiated subtype; diff., differentiating subtype; Intermed., intermediate.
[a]Schneiderman and colleagues [20] also reported 6 cases of MYCN-amplified and favorable histology tumor in favorable stage (A, B, or D). They were included in the reports of Cohn and colleagues [13] and Alvarado and colleagues [19].
[b]These 2 cases were also included in the report by Alvarado and colleagues [19].
[c]This patient experienced tumor progression but was alive at the time of last follow up.

cell type, and prominent nucleoli were not detected in the nuclei of the neuroblastic cells in those cases (Fig. 2).

Immunohistochemically, 3 *MYCN*-A&FH tumors were completely negative for MYCN protein (Fig. 3A), and only a few (<1%) tumor cells in case 2 showed nuclear staining. All negative controls (*MYCN*-nA&FH tumors, *MYCN*-nA&UH tumors, and *MYCN*-A&FH without primary antibody) showed negative staining (Fig. 3B,C), and positive controls (*MYCN*-A&UH tumors) demonstrated positive nuclear staining for MYCN protein (Fig. 3D). As shown in Figure 4, *MYCN* mRNA was not detected by RT-PCR in the tumor of case 1 with appropriate positive controls (*MYCN*-amplified tumor sample and cell line, SK-N-BE [2], both expressing

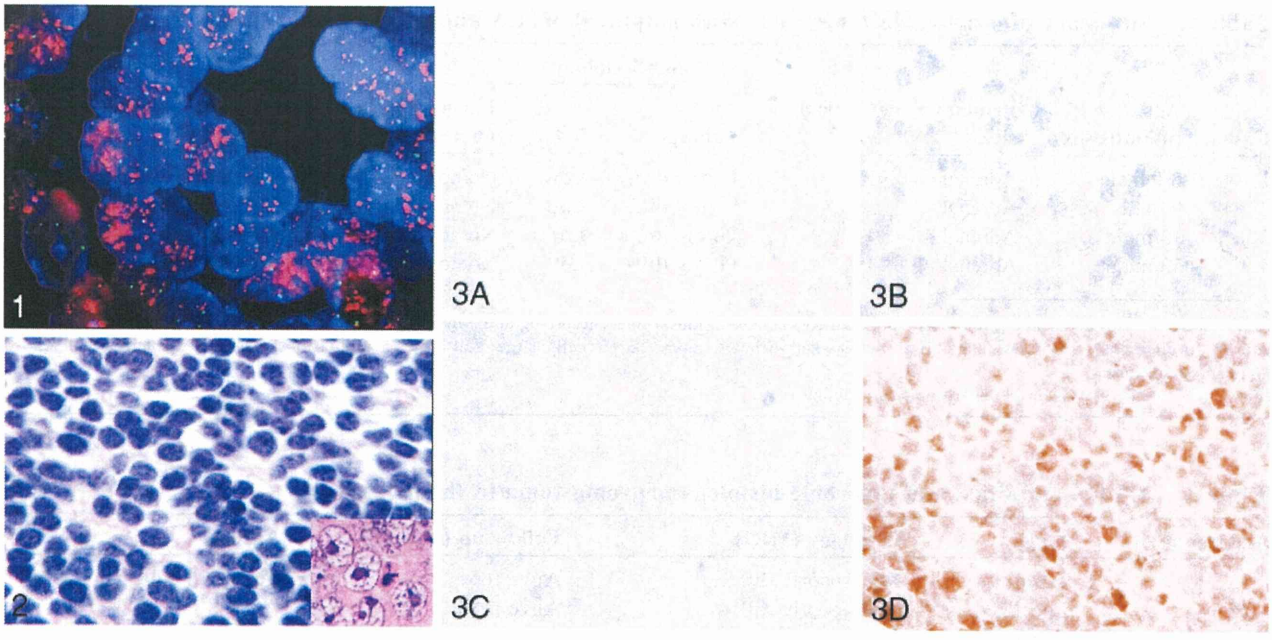

Figure 1. Double staining with *MYCN* probe (orange) and chromosome 2p telomere probe (green). Note numerous orange signals of *MYCN* compared with 2 or 3 green signals of chromosome 2p detected in the individual nuclei of *MYCN*-amplified and favorable histology tumor (case 4, fluorescence in situ hybridization, ×1000).
Figure 2. *MYCN*-amplified and favorable histology tumor showing an appearance of neuroblastoma, poorly differentiated subtype with a low mitosis-karyorrhexis index diagnosed at 6 months of age (case 1, hematoxylin and eosin stain [H&E], ×1000). Inset: Typical morphology of large-cell neuroblastoma with prominent nucleoli in an *MYCN*-amplified and unfavorable histology tumor (case from our file, H&E, ×1000).
Figure 3. Immunohistochemical staining for MYCN protein (×1000). **A.** *MYCN*-amplified and favorable histology tumor from case 1 showing no detectable MYCN protein. **B.** Negative controls of *MYCN*-nonamplified and favorable histology tumor and *MYCN*-nonamplified and unfavorable histology tumor (**C**). **D.** Positive control of *MYCN*-amplified and unfavorable histology tumor showing nuclear staining.

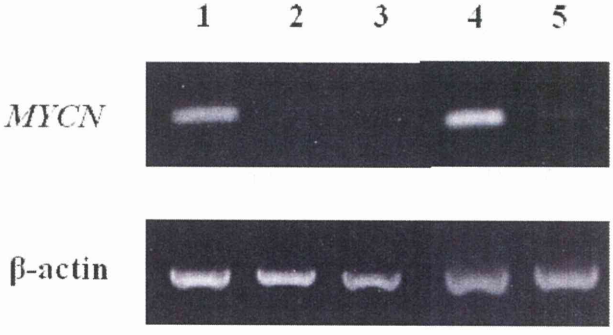

Figure 4. Reverse transcriptase polymerase chain reaction detection of *MYCN* mRNA expression. Lane 1: Positive control, *MYCN*-amplified tumor expressing mRNA. Lane 2: Negative control, *MYCN*-nonamplified tumor expressing no mRNA. Lane 3: *MYCN*-amplified and favorable histology tumor (case 1) expressing no mRNA. Lane 4: Positive control, SK-N-BE(2) (*MYCN*-amplified neuroblastoma cell line) expressing mRNA. Lane 5: Negative control, LA-N-6 (*MYCN*-nonamplified cell line) expressing no mRNA. Cell lines SK-N-BE(2) and LA-N-6 were kindly provided by Dr C.P. Reynolds (Children's Hospital Los Angeles, Los Angeles, CA, USA).

MYCN protein detectable by immunohistochemistry) and negative controls (*MYCN* nonamplified tumor sample and cell line, LA-N-6, both expressing no MYCN protein detectable by immunohistochemistry).

DISCUSSION

MYCN amplification is a well-established molecular indicator for predicting aggressive clinical behavior of NTs [9,10]. *MYCN*-amplified tumors are usually classified into the UH group, according to the INPC. *MYCN* amplification followed by excess MYCN protein expression with subsequent myc-max heterodimer formation in the neuroblastoma cells is considered to be a powerful driving force for preventing cellular differentiation and increasing cellular proliferation (mitosis) and cellular death (karyorrhexis due to DNA instability) [11,12]. Four cases reported here, however, demonstrated a discordant genotype-phenotype relationship. Their tumors had *MYCN* amplification but were classified into the FH group.

Further study demonstrated that MYCN protein was not detected immunohistochemically in our cases. Interpretation of MYCN protein expression by immunohistochemistry requires caution, especially in our 4 tumor samples, which were evaluated as negative. We repeated staining on those tumors and confirmed the results with appropriate positive and negative controls. We also had a chance to perform RT-PCR in 1 case, and no *MYCN* mRNA was detected in the tumor. Cohn and colleagues [13] described similar results of lower or no MYCN protein expression in 2 *MYCN*-A&FH tumors from their

series of 6 cases of *MYCN*-amplified and localized PNTs. One tumor showed a heterogeneous staining pattern by immunohistochemistry, a significantly low expression level by Western blot, and a low expression level of *MYCN* mRNA by Northern blot, and the other showed negative staining immunohistochemically.

To our knowledge, a total of 31 cases of *MYCN*-A&FH neuroblastoma have been reported in detail: 4 cases included in this report and summarized in Table 1 and 27 cases in the literature summarized in Table 2 [13–19]. Schneiderman and colleagues also reported 6 cases of FH&MYCN-amplified tumors from the Pediatric Oncology Group Study [20]. Although they did not mention detailed information of those cases, many of them seemed to be included in the report by Cohn and colleagues [13] and Alvarado and colleagues [19]. Incidence of the MYCN-A&FH tumors in our series (4/63, 6%) was considerably higher than that of the large series (~1%) [12,14]. This was partly because our institutions (Aichi Medical University and the National Center for Child Health and Development) were offering reference diagnostic services for problematic/unusual cases locally and nationally.

Those 31 patients with MYCN-A&FH tumors were diagnosed between age 0.1 and 48 months. The majority (27/31, 87%) were less than 18 months of age. Although follow-up periods of the patients varied, all patients except 2 (20/22, 91%) were alive with localized/nonmetastatic (stage 1, 2, 3) or stage 4S disease. As suggested by Cohn and colleagues [13] and George and colleagues [16], *MYCN*-amplified FH tumors, especially when diagnosed as a localized disease without distant metastasis, would not portend an adverse outcome of the patients. In their report, Schneiderman and colleagues [20] described a relatively low 7-year event-free survival of 50% ± 20% but a higher 7-year overall survival of 83% ± 15% for the patients with FH&MYCN-A tumor in favorable stage (A, B, or D). They also suggested that diploid pattern could be a factor for indicating a poor prognosis of children with MYCN-amplified, favorable-stage neuroblastomas. Each of our 4 cases, including 3 survivors, with MYCN-A&FH tumor in different clinical stages had a diploid pattern. However, 5 of 9 (56%) patients with stage 4 disease died with *MYCN*-A&FH PNTs (Tables 1 and 2).

Several reports describe a significance of prominent nucleoli in MYCN-amplified neuroblastomas [3–6]. Thorner and colleagues [5] pointed out that tumors with macronucleoli were reported as a sign of *MYCN* amplification with a high specificity and a low sensitivity. Sano and colleagues presented a paper at the Advances of Neuroblastoma Research Meeting in 2006 and reported a total of 20 cases of *MYCN*-A&FH neuroblastoma (unpublished results). They distinguished 2 prognostic groups: 1 was composed of conventional FH neuroblastomas (16 cases with 81% 5-year event-free survival and 87% 5-year overall survival), and the other was composed of neuroblastomas of large cell type with prominent nucleoli (4 cases, all died within 13 months from diagnosis). All 4 cases in our series did not have prominent nucleoli and were classified in the conventional FH neuroblastoma group.

We report 4 neuroblastoma cases with amplified *MYCN* and conventional FH, according to the INPC. This is a unique category by combination of unfavorable and favorable prognostic indicators, and 3 of 4 patients in our series are alive and well after high-dose therapy and autologous stem cell rescue. It is speculated that a lack of excess MYCN protein expression despite gene amplification could cause the genotype-phenotype discordance in this rare subset of PTNs. Molecular/genomic alterations other than nonexpression of amplified *MYCN* may also explain the tumors' clinical behavior in our cases. Genome-wide expression analysis would be of interest in this neuroblastoma subtype.

ACKNOWLEDGMENTS

We thank Dr Hiroyuki Shimada (Children's Hospital Los Angeles, Los Angeles, CA, USA) and Dr Hideki Sano (Fukushima Medical University, Fukushima, Japan) for their critical review of the manuscript. We also thank Ms Shino Itoh and Ms Hiromi Ono for their technical assistance.

REFERENCES

1. Shimada H, Ambros IM, Dehner LP, et al. Terminology and morphologic criteria of neuroblastic tumors: recommendations by the International Neuroblastoma Pathology Committee. Cancer 1999;86:349–363.
2. Peuchmaur M, d'Amore ES, Joshi VV, et al. Revision of the International Neuroblastoma Pathology Classification: confirmation of favorable and unfavorable prognostic subsets in ganglioneuroblastoma, nodular. Cancer 2003;98:2274–2281.
3. Kobayashi C, Monforte-Munoz HL, Gerbing RB, et al. Enlarged and prominent nucleoli may be indicative of *MYCN* amplification. Cancer 2005;103:174–180.
4. Tornoczky T, Kalman E, Kajtar P, et al. Large cell neuroblastoma: a distinct phenotype of neuroblastoma with aggressive clinical behavior. Cancer 2004;100:390–397.
5. Thorner PS, Ho M, Chilton-McNeill S, Zielenska M. Use of chromogenic in situ hybridization to identify MYCN gene copy number in neuroblastoma using routine tissue sections. Am J Surg Pathol 2006;30:635–642.
6. Tornoczky T, Semjen D, Shimada H, et al. Pathology of peripheral neuroblastic tumors: significance of prominent nucleoli in undifferentiated/poorly differentiated neuroblastoma. Pathol Oncol Res 2007;13:269–275.
7. Papachristou DJ, Goodman MA, Cieply K, et al. Comparison of allelic losses in chondroblastoma and primary chondrosarcoma of bone and correlation with fluorescence in situ hybridization analysis. Hum Pathol 2006;37:890–898.
8. Gilbert J, Norris MD, Haber M, et al. Determination of *N-myc* gene amplification by differential polymerase chain reaction. Mol Cell Probes 1993;7:227–234.
9. Cohn SL, Tweddle DA. *MYCN* amplification remains prognostically strong 20 years after its "clinical debut." Eur J Cancer 2004;40:2639–2642.
10. Tonini GP, Boni L, Pession A, et al. MYCN oncogene amplification in neuroblastoma is associated with worse prognosis, except in stage 4s: the Italian experience with 295 children. J Clin Oncol 1997;15:85–93.

11. Wenzel A, Czieplunch C, Hamann U, et al. The N-Myc oncoprotein is associated in vivo with the phosphoprotein Max(p20/22) in human neuroblastoma cells. EMBO J 1991;10:3703–3712.
12. Shimada H, Stram DO, Chatten J, et al. Identification of subsets of neuroblastomas by combined histopathologic and N-myc analysis. J Natl Cancer Inst 1995;87:1470–1476.
13. Cohn SL, Look AT, Joshi VV, et al. Lack of correlation of *N-myc* gene amplification with prognosis in localized neuroblastoma: a Pediatric Oncology Group Study. Cancer Res 1995;55:721–726.
14. Goto S, Umehara S, Gerbing RB, et al. Histopathology (International Neuroblastoma Pathology Classification) and *MYCN* status in patients with peripheral neuroblastic tumors: a report from the Children's Cancer Group. Cancer 2001;92:2669–2708.
15. Shimada H, Nakagawa A, Peters J, et al. Trk A expression in peripheral neuroblastic tumors: prognostic significance and biological relevance. Cancer 2004;101:1873–1881.
16. George RE, Variend C, Cullinane SJ, et al. Relationship between histological features, MYCN amplification, and prognosis: a UKCCSG Study. Med Pediatr Oncol 2001;36:169–176.
17. Fabbretti G, Valenti C, Loda M, et al. *N-myc* gene amplification/expression in localized stroma-rich neuroblastoma (ganglioneuroblastoma). Hum Pathol 1993;24:294–297.
18. Perez CA, Matthay KK, Atkinson JB, et al. Biologic variables in the outcome of stages I and II neuroblastoma treated with surgery as primary therapy: a Children's Cancer Group report. J Clin Oncol 2000;18:18–26.
19. Alvarado CS, London WB, Look AT, et al. Natural history and biology of stage A neuroblastoma: a Pediatric Oncology Group Study. J Pediatr Hematol Oncol 2000;22:197–205.
20. Schneiderman J, London WB, Brodeur GM, et al. Clinical significance of MYCN amplification and ploidy in favorable-stage neuroblastoma: a report from the Children's Oncology Group. J Clin Oncol 2008;26:913–918.

Published OnlineFirst September 9, 2011; DOI:10.1158/1078-0432.CCR-11-0313

Clinical Cancer Research

Expression of *NLRR3* Orphan Receptor Gene Is Negatively Regulated by MYCN and Miz-1, and Its Downregulation Is Associated with Unfavorable Outcome in Neuroblastoma

Jesmin Akter, Atsushi Takatori, Md. Shamim Hossain, et al.

Clin Cancer Res 2011;17:6681-6692. Published OnlineFirst September 9, 2011.

Published OnlineFirst September 9, 2011; DOI:10.1158/1078-0432.CCR-11-0313

Human Cancer Biology

Clinical Cancer Research

Expression of *NLRR3* Orphan Receptor Gene Is Negatively Regulated by MYCN and Miz-1, and Its Downregulation Is Associated with Unfavorable Outcome in Neuroblastoma

Jesmin Akter[1,2], Atsushi Takatori[1], Md. Shamim Hossain[1], Toshinori Ozaki[1,3], Atsuko Nakazawa[5], Miki Ohira[4], Yusuke Suenaga[1], and Akira Nakagawara[1,2]

Abstract

Purpose: Our previous study showed that expression of NLRR3 is significantly high in favorable neuroblastomas (NBL), whereas that of NLRR1 is significantly high in unfavorable NBLs. However, the molecular mechanism of transcriptional regulation of *NLRR3* remains elusive. This study was undertaken to clarify the transcriptional regulation of *NLRR3* and its association with the prognosis of NBL.

Experimental Design: *NLRR3* and *MYCN* expressions in NBL cell lines were analyzed after induction of cell differentiation, MYCN knockdown, and overexpression. The transcriptional regulation of *NLRR3* was analyzed by luciferase reporter and chromatin immunoprecipitation assays. Quantitative PCR was used for examining the expression of *NLRR3*, *Miz-1*, or *MYCN* in 87 primary NBLs.

Results: The expression of *NLRR3* mRNA was upregulated during differentiation of NBL cells induced by retinoic acid, accompanied with reduced expression of *MYCN*, suggesting that *NLRR3* expression was inversely correlated with *MYCN* in differentiation. Indeed, knockdown of *MYCN* induced *NLRR3* expression, whereas exogenously expressed MYCN reduced cellular *NLRR3* expression. We found that Miz-1 was highly expressed in favorable NBLs and *NLRR3* was induced by *Miz-1* expression in NBL cells. MYCN and Miz-1 complexes bound to *NLRR3* promoter and showed a negative regulation of *NLRR3* expression. In addition, a combination of low expression of *NLRR3* and high expression of *MYCN* was highly associated with poor prognosis.

Conclusions: *NLRR3* is a direct target of MYCN, which associates with Miz-1 and negatively regulates *NLRR3* expression. NLRR3 may play a role in NBL differentiation and the survival of NBL patients by inversely correlating with *MYCN* amplification. *Clin Cancer Res; 17(21); 6681–92. ©2011 AACR.*

Introduction

Neuroblastoma (NBL) is one of the most common malignant solid tumors in children and accounts for 8% of all pediatric cancers (1). NBLs originate from sympathetic precursor neuroblasts derived from the neural crest. NBLs found in patients older than 1 year are usually aggressive and eventually kill the patients despite intensive therapy, whereas those in patients younger than 1 year often regress spontaneously or maturate, resulting in a favorable prognosis (2). We have made extensive efforts to show that TrkA, a high-affinity receptor for nerve growth factor, and TrkB, a receptor for brain-derived neurotrophic factor as well as neurotrophin 4/5, are important key regulators (3–6). However, the precise molecular mechanisms of how NBL becomes aggressive and how the spontaneous regression is induced still remain elusive.

Amplification of the *MYCN* oncogene is strongly associated with rapid progression of NBL (7). The *MYCN* amplification occurs in approximately 25% of NBL and is one of the most important prognostic indicators of poor clinical outcome (8–12). MYCN is a nuclear transcription factor and its expression level is well associated with cell proliferation of NBL cells (13, 14). In general, MYCN exerts its biological functions through transcriptional regulation of its target genes in both positive and negative manners. MYCN has an ability to activate its target genes by forming a heterodimer with MAX and binds to the E-box motif, CACGTG, in the proximal promoter region (15–18). On the contrary, MYCN represses the expression of genes, such

Authors' Affiliations: [1]Division of Biochemistry and Innovative Cancer Therapeutics, Chiba Cancer Center; [2]Department of Molecular Biology and Oncology, Chiba University Graduate School of Medicine; [3]Laboratories of Anti-Tumor Research and [4]Cancer Genomics, Chiba Cancer Center Research Institute, Chiba; and [5]Department of Pathology, National Center for Child Health and Development, Tokyo, Japan

Note: Supplementary data for this article are available at Clinical Cancer Research Online (http://clincancerres.aacrjournals.org/).

Corresponding Author: Akira Nakagawara, Division of Biochemistry and Innovative Cancer Therapeutics, Chiba Cancer Center, 666-2 Nitona, Chuoh-ku, Chiba 260-8717, Japan. Phone: 81-43-264-5431; Fax: 81-43-265-4459; E-mail: akiranak@chiba-cc.jp

doi: 10.1158/1078-0432.CCR-11-0313

Published OnlineFirst September 9, 2011; DOI:10.1158/1078-0432.CCR-11-0313

Translational Relevance

Amplification of *MYCN* oncogene is strongly associated with rapid progression of neuroblastoma (NBL) and one of the most important prognostic indicators of poor clinical outcome. Our group previously reported that NLRR3 is highly expressed in a favorable subset of NBL but until this work, there was no sound investigation of the function of NLRR3 and its transcriptional regulation. In this study, we found that *NLRR3* is a direct target of MYCN but its expression is negatively regulated by MYCN in association with Miz-1. Furthermore, a combination of low expression level of *NLRR3* and high expression level of *MYCN* was strongly correlated with the poor prognosis. These data suggest that the expression pattern of NLRR3, Miz-1, and MYCN plays an important role in defining the clinical behavior of NBLs. The decreased expression of NLRR3 might be one of the key events regulating the aggressive behavior of NBL.

as $p15^{INK4b}$, $p21^{CIP1}$, and *NDRG2*, when it forms a complex with transcriptional regulators, such as Myc-interacting zinc finger protein 1 (Miz-1) and Sp1 (19–21). Koppen and colleagues have previously described that MYCN suppresses *Dickkopf-1* (*DKK1*) expression, resulting in proliferation of NBL cells (22). However, the precise mechanism of how MYCN contributes to NBL aggressiveness remains unclear.

We have identified human neuronal leucine-rich repeat (NLRR) family genes as one of the differentially expressed genes between favorable and unfavorable NBLs, using our unique NBL cDNA libraries (23, 24). The NLRR protein family consists of 3 members, NLRR1, NLRR2, and NLRR3 (23), and belongs to the type γ transmembrane protein with leucine-rich repeat (LRR) domains containing 11 or 12 LRRs, an immunoglobulin c2-type domain, and a fibronectin type III domain in its extracellular region. The amino acid sequences of NLRR family proteins are highly conserved in the extracellular domains, and NLRR1 and NLRR3 also possess a conserved stretch of 11 amino acids with 2 clathrin adapter interaction domains and a dileucine-type domain in the short intracellular region (25, 26), which might provide a basis for NLRR function. Our previous reports showed that NLRR1 is a direct transcriptional target of MYCN and that a high expression level of *NLRR1* mRNA is associated with a poor prognosis of NBL (23, 27). However, the function of NLRR3 is poorly understood except that mouse *NLRR3* expression is increased in the cerebral cortex after a cortical brain injury (28) and that rat NLRR3 may be involved in the regulation of EGF receptor signaling through interaction with clathrins (26).

We have previously reported that high levels of *NLRR3* mRNA expression are associated with favorable prognostic factors in NBL (23). In this study, we found that NLRR3 is induced during differentiation of NBL cells. Transcriptional analysis has revealed that NLRR3 is a direct transcriptional target of MYCN, which negatively transactivates it in association with Miz-1. Furthermore, high expression of *NLRR3* or *Miz-1* and the combination of high expression of both *NLRR3* and *Miz-1* are significantly associated with a favorable outcome of NBL. On the contrary, the low expression levels of *NLRR3* and high expression of *MYCN* were strongly correlated with a poor prognosis of NBL.

Materials and Methods

Patient population

Eighty-seven patients with NBL were diagnosed clinically and histologically, using a surgically removed tumor specimen according to the International Neuroblastoma Pathological classification (INPC). According to the International NBL Staging System (INSS; ref. 29), 18 patients were diagnosed as stage 1, 11 were stage 2, 20 were stage 3, 33 were stage 4, and 5 were stage 4S. Cytogenetic and molecular biological analysis of all tumors was also carried out by assessing DNA ploidy, *MYCN* amplification, and *TrkA* expression. The patients were then treated following the protocols proposed by the Japanese Infantile NBL Cooperative Study (30) and Group for Treatment of Advanced NBL (31), and subjected to survival analysis of the result in a follow-up period of at least 36 months (range, 4–58). The study was conducted under internal review board approval with appropriate informed consent.

Cell lines and transient transfection

Human NBL-derived cell lines, including SK-N-BE, CHP134, IMR32, GOTO, KAN, KP-N-NS, LAN-5, NB-1, NB-9, NLF, RTBM1, SK-N-DZ, TGW, NB69, NBL-S, OAN, SK-N-AS, SK-N-SH, and SH-SY5Y cells were obtained from the CHOP cell line bank (Philadelphia, PA) and maintained in a culture condition, using RPMI 1640 supplemented with 10% heat-inactivated FBS (Invitrogen), 100 IU/mL penicillin, and 100 μg/mL streptomycin in a 37°C, 5% CO_2 incubator. For the NBL cell differentiation experiment, RTBM1 and SH-SY5Y cells were exposed to all-*trans* retinoic acid (ATRA; Sigma) at a final concentration of 5 μmol/L. For transient transfection, cells were transfected with the indicated expression of plasmids by using a Lipofectamine 2000 transfection reagent (Invitrogen), according to the manufacturer's recommendations.

RNA extraction and semiquantitative reverse transcriptase PCR

Total RNA was prepared from fresh-frozen tissues of primary NBLs or cultured cells by using Trizol reagents (Life Technologies) or the RNeasy Mini kit (Qiagen). Reverse transcription was carried out by random primers and Superscript II (Invitrogen), following the manufacturer's instructions. After reverse transcription, the resultant cDNA was subjected to PCR-based amplification. The sequence of the primer sets were used for PCR amplification is listed in the Supplementary Table S4. All PCR amplifications were carried out with a GeneAmp PCR 9700 (Perkin-Elmer Co), using rTaq DNA polymerase (Takara).

Published OnlineFirst September 9, 2011; DOI:10.1158/1078-0432.CCR-11-0313

The expression of *GAPDH* was measured as an internal control.

Quantitative real-time PCR

cDNA from primary NBLs and cell lines were subjected to the real-time PCR to quantitate the expression levels of *MYCN*, *Miz-1*, and *NLRR3* mRNA. TaqMan GAPDH control reagent kit (Perkin-Elmer Applied Biosystems) was used for *GAPDH* expression and analyzed by an ABI prism 7500 Sequence Detection System (Applied Biosystems). *NLRR3* and *Miz-1* TaqMan probes were purchased from Applied Biosystems. *MYCN* mRNA expression was measured by the SYBR green real-time PCR system. The primers and probes used for real-time PCR were listed in Supplementary Table S4.

Generation of a specific antibody against NLRR3

The rabbit polyclonal anti-NLRR3 antibody was raised against a mixed synthetic peptide corresponding to amino acid sequences between positions 655 to 670 and 692 to 707 of human NLRR3. The peptide and polyclonal antibody (TB0266) were generated by Medical and Biological Laboratories (Nagoya, Japan). The specificity of the affinity-purified antibody was assayed by immunoblotting.

Plasmid constructs

The protein-coding region of *Miz-1* was amplified by PCR and inserted into the *Eco*RI site of pcDNA3.1 (Invitrogen) flanked with a Flag tag. The human *NLRR3* promoter region and its 5′ progressive deletion mutant were amplified by PCR and then inserted into the *Sacy* site in the upstream of the luciferase gene of the pGL3-basic plasmid (Promega). All constructs were verified by DNA sequencing. The pUHD-MYCN vector was kindly provided by Dr. M. Schwab (German Cancer Research Center, Heidelberg, Germany).

Luciferase reporter assay

SH-SY5Y cells were seeded at a density of 5×10^4 cells/12-well cell culture plate and allowed to attach overnight. The cells were transiently cotransfected with each mutant of the human *NLRR3* promoter-driven luciferase reporter and an internal control vector for *Renilla* luciferase, or a combination of the indicated expression vectors. The total amount of plasmid DNA per transfection was kept consistent with the pcDNA3.1 vector. Both firefly and *Renilla* luciferase activities were assayed with the Dual-Luciferase reporter assay system (Promega) according to the manufacturer's instructions. The firefly luminescence signal was normalized on the basis of the *Renilla* luminescence signal.

siRNA transfection

To knockdown endogenous MYCN expression, SK-N-AS, SK-N-BE, and SH-SY5Y cells were transfected with 10 nmol/L of the indicated siRNA purchased from Dharmacon by using LipofectAMINE RNAiMAX (Invitrogen), according to the manufacturer's recommendations. The list of siRNA sequences used will be provided upon request. Forty-eight hours after transfection, cell lysates were prepared and analyzed for the expression levels of NLRR3 and MYCN by immunoblotting.

Immunoblot analysis

The cells were washed twice with ice-cold PBS and then lysed immediately with SDS sample buffer containing 10% glycerol, 5% β-mercaptoethanol, 2.3% SDS, and 62.5 mmol/L Tris-HCl (pH 6.8). The protein concentrations were determined by using Bio-Rad protein assay dye reagent (Bio-Rad Laboratories). Equal amounts of cell lysates were separated by SDS-PAGE and electrophoretically transferred onto Immobilon-P membranes (Millipore). The transferred membranes were blocked with 5% nonfat dry milk in TBS containing 0.1% Tween-20 and incubated with appropriate primary antibodies at room temperature for 1 hour followed by incubation with horseradish peroxidase–conjugated goat anti-mouse or anti-rabbit secondary antibodies (Cell Signaling Technology Inc.) at room temperature for 1 hour. Immunoreactive bands were visualized by an ECL system (GE Healthcare). The primary antibodies used in this study were as follows: monoclonal anti-MYCN (Ab-1; Oncogene Research Products), polyclonal anti-NLRR3, polyclonal anti–Miz-1 (Santa Cruz Biotechnology), monoclonal anti-GAP43 (9-1E21; Chemicon), and polyclonal anti-actin (20-33; Sigma) antibodies.

Chromatin immunoprecipitation assays

A chromatin immunoprecipitation (ChIP) assay was carried out according to the protocol provided by Upstate Biotechnology (Charlottesville). In brief, cells were cross-linked with 1% formaldehyde in medium for 10 minutes at 37°C. Chromatin solutions were prepared and immunoprecipitated with the following antibodies: anti-MYCN, anti–Miz-1, anti-Max rabbit polyclonal antibodies (Santa Cruz Biotechnology), and normal mouse or rabbit serum as a control. The immunoprecipitates were eluted with 100 μL of elution buffer (1% SDS and 1 mmol/L $NaHCO_3$). Formaldehyde-mediated cross-links were reversed by heating at 65°C for 4 hours, and the reaction mixtures were treated with proteinase K at 45°C for 1 hour. DNAs of the immunoprecipitates and control input DNAs were purified by using a QIAquick PCR purification kit (Qiagen). Purified DNA was subjected to optimized semiquantitative PCR amplification protocol for NLRR3 gene promoter and control regions, using appropriate primer sets (Supplementary Table S4).

Statistical analysis

Student *t* tests were employed to examine the possible association between *NLRR3* expression and other prognostic factors. The classification of high and low levels of *NLRR3*, *Miz-1*, and *MYCN* expression was determined on the basis of the mean value obtained from quantitative real-time PCR analysis. Kaplan–Meier survival curves were calculated, and survival distributions were compared by using the log-rank test. Cox regression models were used to search associations along with *NLRR3* expression, *MYCN*

Published OnlineFirst September 9, 2011; DOI:10.1158/1078-0432.CCR-11-0313

expression, *Miz-1* expression, age, *MYCN* amplification status, INSS, *TrkA* expression, DNA index, origin, and survival. Statistical significance was considered if P value was less than 0.05. The statistical analysis was carried out by SPSS Statistical Software release 12.0.

Results

NLRR3 is upregulated during neuronal differentiation

It has been previously reported that the NBL cell lines exposed to ATRA undergo neuronal differentiation (32), accompanied by a marked decrease in the expression levels of *MYCN* (33). To examine the possible involvement of MYCN in the regulation of NLRR3 expression, the NBL-derived RTBM1 cells were treated with or without 5 μmol/L ATRA. As previously described (34), RTBM1 cells underwent neuronal differentiation with extensive neurite outgrowth in response to ATRA treatment (Fig. 1A). The induced differentiation was confirmed by the expression levels of *GAP43*, a marker of neuronal differentiation (35), which increased after ATRA treatment at both mRNA and protein levels (Fig. 1B and C). As expected, MYCN expression was significantly decreased after ATRA treatment and almost diminished at 6 days after treatment. Consistent with our previous observations (23), *NLRR3* was markedly upregulated at the mRNA and protein levels during the differentiation process. Similar results were also obtained from ATRA-treated SH-SY5Y cells (Supplementary Fig. S1A and B).

Inverse correlation between *MYCN* and *NLRR3* expressions

To further confirm a possible relationship between MYCN and NLRR3, we used MYCN-inducible SHEP21N cells originally derived from NBL (36) and treated with tetracycline to switch off the expression of MYCN. As shown in Fig. 2A, the reduced expression level of *MYCN* upon tetracycline treatment was confirmed by reverse transcriptase PCR (RT-PCR) and immunoblotting, whereas NLRR3 expression was increased after tetracycline treatment.

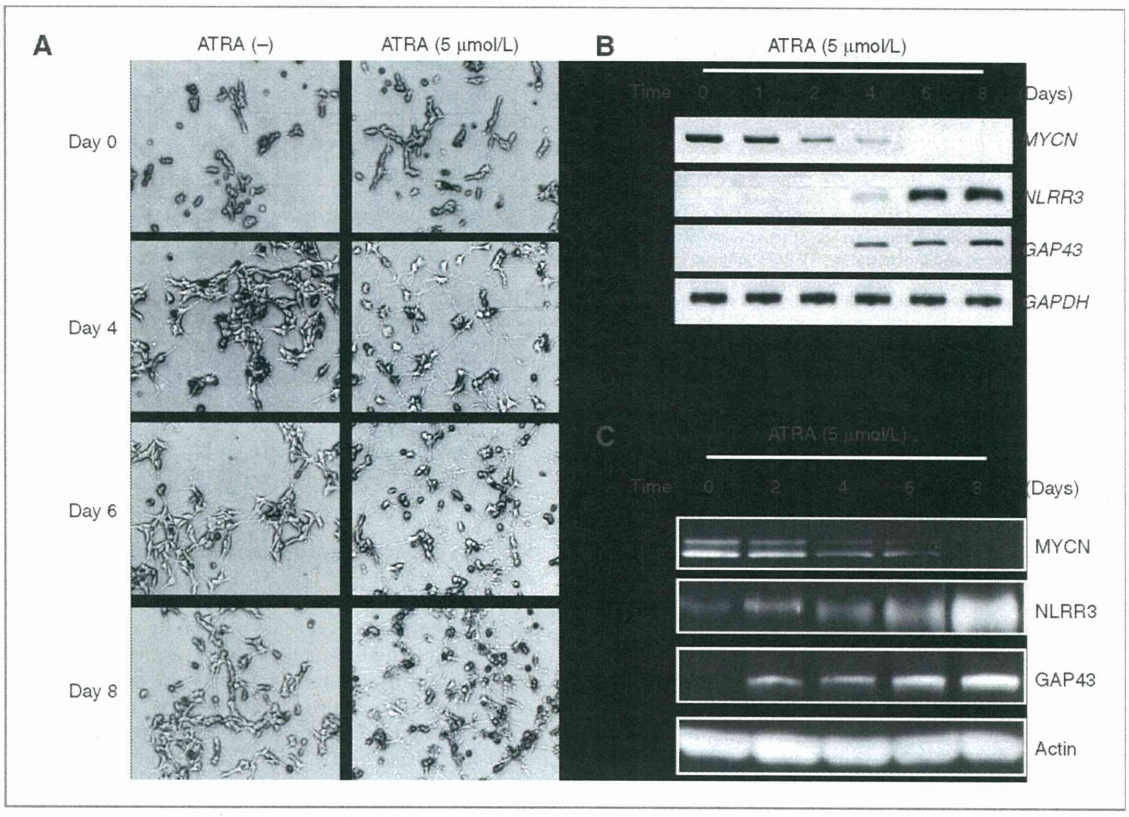

Figure 1. Opposite expression pattern of *NLRR3* and *MYCN* in differentiated RTBM1 cells in response to ATRA. A, ATRA-induced differentiation program in RTBM1 cells. Cells were treated with 5 μmol/L ATRA or left untreated. At the indicated time-periods after treatment with ATRA, neurite outgrowth was examined with a phase-contrast microscope. B and C, RT-PCR and immunoblot analysis for MYCN, NLRR3, and GAP43 in response to ATRA. RTBM1 cells were treated as in A. Total RNA and cell lysates were prepared and processed for RT-PCR (B) and immunoblotting with indicated antibodies (C). For RT-PCR, *GAPDH* was used as an internal control. For immunoblotting, actin was used as a loading control.

Published OnlineFirst September 9, 2011; DOI:10.1158/1078-0432.CCR-11-0313

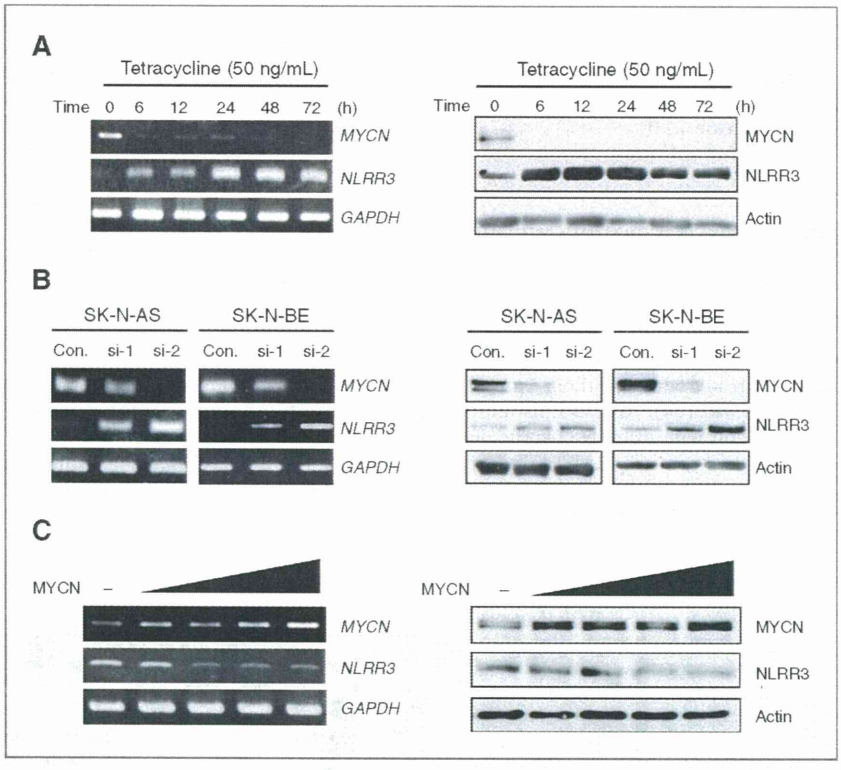

Figure 2. Inverse regulation of MYCN and NLRR3 in various NBL cell lines. A, RT-PCR and immunoblot analysis for MYCN and NLRR3 in SHEP21N cells maintained in the presence of tetracycline. At the indicated time points after the addition of tetracycline (50 ng/mL), total RNA and cell lysates were prepared and processed for RT-PCR (left) and immunoblotting with indicated antibodies (right). B, siRNA-mediated knockdown of the endogenous MYCN. SK-N-AS and SK-N-BE cells were transfected with control siRNA (Con.) or with 2 siRNA (si-1 and si-2) against MYCN. At 48 hours after transfection, total RNA and cell lysates were prepared and processed for RT-PCR (left) and immunoblotting with indicated antibodies (right). C, SH-SY5Y cells were transiently transfected with or without the increasing amounts of the expression plasmid encoding MYCN. Forty-eight hours after transfection, total RNA and cell lysates were prepared and processed for RT-PCR (left) and immunoblotting (right) with indicated antibodies. *GAPDH* was used as an internal control of RT-PCR and actin was used as a loading control for immunoblotting.

To examine whether MYCN and NLRR3 have an inverse functional relationship under these physiologic conditions, siRNA knockdown of the endogenous MYCN was carried out in 2 NBL cell lines, SK-N-AS cells with a single copy of *MYCN* and SK-N-BE cells with *MYCN* amplification. As shown in Fig. 2B, one of the siRNAs against *MYCN*, si-2, efficiently reduced endogenous expression of *MYCN* in both cell lines and resulted in an increased expression of NLRR3. SH-SY5Y cells with a single copy of *MYCN* also showed the similar result after siRNA-mediated knockdown of the endogenous MYCN (Supplementary Fig. S2A and B). These observations prompted us to examine whether MYCN can directly downregulate *NLRR3* expression. To address this issue, SH-SY5Y NBL cells were transfected with the expression plasmid encoding the *MYCN* gene. Forced expression of MYCN resulted in a dose-dependent decrease of NLRR3 expression both at the mRNA and protein levels (Fig. 2C), suggesting that *NLRR3* expression is negatively regulated by MYCN in NBL cells.

MYCN represses the promoter activity of *NLRR3* in association with Miz-1

According to the previous reports (19, 20, 37), Myc proteins repress its target genes by forming a complex with Miz-1. Under these conditions at low expression levels of Myc, Miz-1 activates transcription of the target genes by cooperating with other transcriptional cofactors and enhances cell differentiation (20). Therefore, we hypothesized that Miz-1 might be involved in the regulation of *NLRR3* expression. To prove this, we examined whether exogenously expressed Miz-1 upregulates *NLRR3* expression in SH-SY5Y cells. Figure 3A, left shows that *NLRR3* expression was upregulated by overexpression of Miz-1 in the same manner as a positive control, $p15^{Ink4b}$ expression, whereas expression of other NLRR family members, *NLRR1*

Published OnlineFirst September 9, 2011; DOI:10.1158/1078-0432.CCR-11-0313

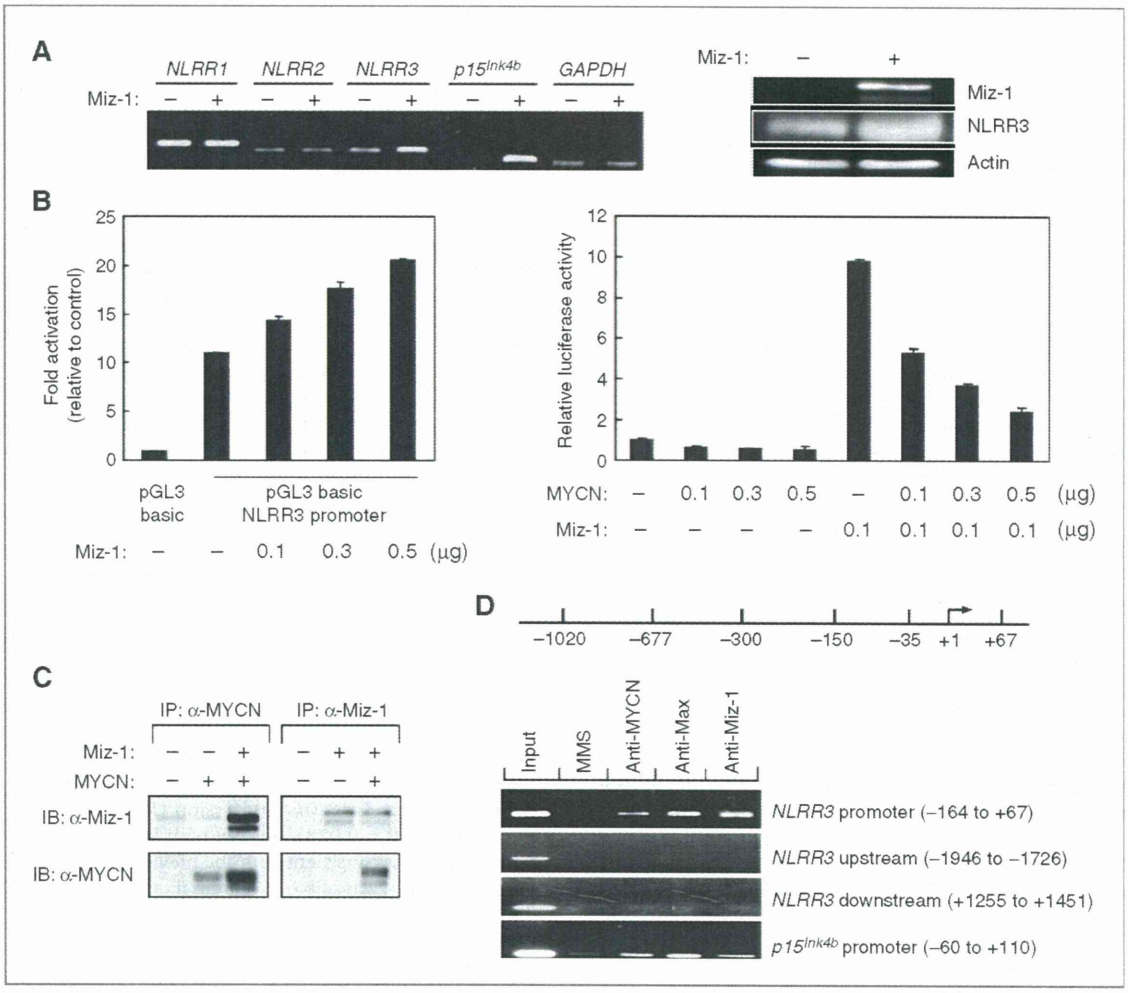

Figure 3. Regulation of the *NLRR3* promoter by MYCN and Miz-1. A, left, RT-PCR analysis showing expression of *NLRR1*, *NLRR2*, *NLRR3*, and $p15^{INk4b}$ in SH-SY5Y cells transiently transfected either with control or Miz-1–expressed plasmid. *GAPDH* was used as an internal control. Right, Western blot showing expression of *NLRR3* and *Miz-1* in SH-SY5Y cells transiently transfected either with control vector or with Miz-1 expressing vector. Actin was used as a loading control. B, left, Miz-1 enhances promoter activity of *NLRR3* in transient transfection assay. Data represent fold activation of the *NLRR3* promoter (−677 to +67) construct upon coexpression of increasing amounts of the expression plasmid for Miz-1 in SY5Y cells. Forty-eight hours after transfection, the cells were lysed and their relative luciferase activities were measured. Firefly luminescence signal was normalized on the basis of *Renilla* luminescence signal. Right, expression of MYCN reduces the basal activity of the *NLRR3* promoter and abrogates transactivation by Miz-1. SH-SY5Y cells were transiently cotransfected with or without constant amount of the expression plasmid for the Miz-1 and 0.1 μg of *NLRR3* promoter (−677 to +67) together with or without the increasing amounts of the expression plasmid for MYCN. The luciferase activity was determined as in B, left. Results are the mean of 3 independent experiments ± SD. C, interaction between MYCN and Miz-1 in NBL cells. Whole cell lysates prepared from SK-N-AS cells transfected with indicated vectors and immunoprecipitated (IP) with the monoclonal anti-MYCN antibody or with polyclonal anti–Miz-1 antibody. The immunoprecipates were analyzed by immunoblotting (IB) with the polyclonal anti–Miz-1 antibody or with monoclonal anti-MYCN antibody, respectively. D, ChIP analysis of SH-SY5Y cells was carried out by using the indicated antibody and PCR primers specific for the different part of *NLRR3* promoter (top 3 panels), upstream, downstream (middle 2 panels) regions of the *NLRR3* gene, and for $p15^{INk4b}$ promoter (bottom).

and *NLRR2*, showed no change. The increased expression of NLRR3 protein was also confirmed by Western blot analysis (Fig. 3A, right). This induction of NLRR3 by Miz-1 was also observed in SK-N-AS cells (Supplementary Fig. S3). To determine whether Miz-1 activates the *NLRR3* promoter, the region spanning exon 2 and 5′-upstream sequences of the *NLRR3* gene (nucleotide −1,020 to +67) was cloned and analyzed for promoter activity by using a luciferase reporter assay. The promoter deletion analysis showed that a nucleotide position between −677 and +67 gives maximum promoter activity (Supplementary Fig. S4A). The core promoter region (−35 to +67) also

Published OnlineFirst September 9, 2011; DOI:10.1158/1078-0432.CCR-11-0313

showed higher promoter activity than other deletion mutants. In transient-cotransfection assays, simultaneous expression of Miz-1 increased the luciferase activities driven by the *NLRR3* promoter (−677 to +67; Fig. 3B, left).

On the contrary, overexpression of MYCN resulted in reduced activity of the *NLRR3* promoter (Supplementary Fig. S4B). These results suggest that Miz-1 and MYCN together contribute to the transcriptional regulation of the *NLRR3* gene. Indeed, the activation of the *NLRR3* promoter by exogenous Miz-1 expression in SH-SY5Y cells was suppressed by coexpression of MYCN in a dose-dependent manner (Fig. 3B, right). The luciferase activities driven by the core promoter region (−35 to +67) also showed a similar result (data not shown). It was reported that a transcriptional suppression of the MYCN-targeted genes occurs when MYCN forms a complex with Miz-1 and Max (19). To make certain of the physical interaction between MYCN and Miz-1, the whole cell lysates prepared from the SK-N-AS cells cotransfected with *MYCN* and *Miz-1* were subjected to an immunoprecipitation assay. As shown in Fig. 3C, coimmunoprecipitation using either MYCN or Miz-1 antibody confirmed that MYCN and Miz-1 formed a complex in SK-N-AS cells as previously reported in non-NBL cell lines (38). Moreover, ChIP analysis revealed that MYCN, Max, and Miz-1 were recruited onto the same promoter region of *NLRR3* (−164 to +67) in SH-SY5Y cells (Fig. 3D). Hence, MYCN negatively regulates *NLRR3* expression by forming a transcriptional complex with Miz-1 in NBL cells.

Increased expression of *NLRR3* and *Miz-1* in favorable neuroblastoma

In our previous report, *NLRR3* is highly expressed in favorable NBLs with a single copy of *MYCN* as compared with NBLs with *MYCN* amplification. To evaluate whether the expression pattern of *Miz-1*, *NLRR3*, and *MYCN* observed in NBL cell lines is consistent in primary NBLs, we analyzed expression levels of those 3 genes in 16 favorable (stages 1 or 2, high expression of *TrkA* and a single copy of *MYCN*) and 16 unfavorable (stages 3 or 4, low expression of TrkA and amplification of *MYCN*) NBL samples by semiquantitative RT-PCR. As shown in Supplementary Fig. S5A, *NLRR3* and *Miz-1* were expressed at higher levels in favorable NBLs than those in unfavorable tumors, whereas the levels of *MYCN* expression were predominantly high in the unfavorable tumors. The expression levels of *NLRR3* and *Miz-1* were also higher in the cell lines with a single copy of *MYCN* than those with *MYCN* amplification, indicating evidence of a positive correlation between *NLRR3* and *Miz-1* expressions and of an inverse correlation between *NLRR3* and *MYCN* expressions (Supplementary Fig. S5B). Those expression patterns were further assessed by immunohistochemistry for NLRR3, MYCN, and Miz-1 in primary NBL tissues (Supplementary Fig. S5C). We carried out immunohistochemical staining on all 11 available paraffin-embedded primary NBL tissues, including 5 NBLs with a single copy of *MYCN* and favorable histology according to INPC (39), 3 NBLs carrying a single copy of *MYCN* with unfavorable histology, and 3 NBLs with *MYCN* amplification and unfavorable histology. As shown in Supplementary Fig. S5C and Supplementary Table S1, the absence of MYCN amplification was associated with strong positive staining of NLRR3 and Miz-1 in all examined samples except one (case 8). All 3 NBLs with *MYCN* amplification showed weak staining for both NLRR3 and Miz-1.

Low expression of *NLRR3* and *Miz-1* is associated with an unfavorable outcome of neuroblastoma

To evaluate whether a statistically significant relationship exists between the patients' survival periods and the expression of *NLRR3*, *Miz-1*, or *MYCN* in primary NBLs, we quantitatively measured the expression levels of *NLRR3*, *Miz-1*, and *MYCN* mRNAs in 87 primary NBLs by using the quantitative real-time PCR method. The clinical features of each NBL samples are listed in Supplementary Table S2. As shown in Table 1, high levels of *NLRR3* expression were significantly associated with younger age ($P = 0.047$), single copy of *MYCN* ($P = 0.047$), favorable disease stages ($P = 0.041$), high levels of *TrkA* expression ($P = 0.042$), and diploid DNA index ($P = 0.003$), but not with tumor origin ($P = 0.933$). A high level of *Miz-1* expression was also significantly associated with younger age ($P = 0.004$), single copy of *MYCN* ($P = 0.004$), favorable disease stages ($P = 0.001$), and high levels of *TrkA* expression ($P = 0.001$), but not with DNA index ($P = 0.060$) and tumor origin ($P = 0.959$). In contrast, a high level of *MYCN* expression was significantly associated with *MYCN* amplification ($P = 0.0001$), advanced disease stages ($P = 0.0031$), low levels of *TrkA* expression ($P = 0.026$), and tumor origin ($P = 0.028$), but not with DNA index ($P = 0.079$), which is consistent with the previous reports (23, 40, 41). There was also a marginal association with patient age ($P = 0.063$). These results suggest that high expression of *NLRR3* and *Miz-1* is well associated with conventional prognostic markers predicting a favorable NBL outcome.

To examine whether the expression levels of *NLRR3*, *Miz-1* and/or *MYCN* have a prognostic significance in primary NBLs, we employed log-rank tests for gene-expression data (Supplementary Table S3). There were significant differences in survival rates in the groups of patients with high and low expression of *NLRR3*, *Miz-1*, and *MYCN*. Patients with high expression of *NLRR3* or *Miz-1* had a higher survival rate than patients with low expression of *NLRR3* or *Miz-1*, and such a difference in survival rate was statistically significant ($P = 0.0023$ and $P = 0.00060$, respectively). However, a patient with high *MYCN* expression was associated with a lower survival rate than that of the *MYCN* low subset ($P < 0.00001$; Supplementary Table S3). Figure 4 shows Kaplan–Meier cumulative survival curves for 87 patients with NBL in terms of expression of *NLRR3*, *Miz-1* and *MYCN*. High expression of *NLRR3* and that of *Miz-1* were significantly associated with good survival ($P = 0.0023$ and $P = 0.00060$, respectively; Fig. 4A, left and right). As already known, high expression of *MYCN*

Published OnlineFirst September 9, 2011; DOI:10.1158/1078-0432.CCR-11-0313

Table 1. Correlation between expression of *NLRR3* or *MYCN* or *Miz-1* and other prognostic factors (Student *t* test)

		NLRR3		*MYCN*		*Miz-1*	
Variable	**No.**	**Mean ± SEM**	***P***	**Mean ± SEM**	***P***	**Mean ± SEM**	***P***
Age, y							
<1	32	0.043 ± 0.011	0.047[a]	0.034 ± 0.013	0.063	0.091 ± 0.019	0.004[a]
≥1	55	0.024 ± 0.003		0.141 ± 0.043		0.042 ± 0.007	
MYCN copy number							
Single copy	58	0.041 ± 0.006	0.047[a]	0.022 ± 0.016	0.0001[a]	0.077 ± 0.012	0.004[a]
Amplified	29	0.019 ± 0.004		0.222 ± 0.053		0.026 ± 0.004	
Tumor stage							
1, 2, 4s	34	0.043 ± 0.009	0.041[a]	0.007 ± 0.002	0.0031[a]	0.093 ± 0.017	0.001[a]
3, 4	53	0.024 ± 0.003		0.144 ± 0.036		0.039 ± 0.007	
TrkA expression							
High	24	0.047 ± 0.013	0.042[a]	0.009 ± 0.003	0.026[a]	0.104 ± 0.024	0.001[a]
Low	61	0.025 ± 0.004		0.125 ± 0.032		0.044 ± 0.006	
DNA index							
Diploidy	42	0.019 ± 0.003	0.003[a]	0.121 ± 0.037	0.079	0.049 ± 0.008	0.06
Aneuploidy	31	0.050 ± 0.010		0.034 ± 0.023		0.085 ± 0.019	
Tumor origin							
Adrenal gland	48	0.032 ± 0.007	0.933	0.135 ± 0.035	0.028[a]	0.059 ± 0.012	0.959
Others	39	0.032 ± 0.004		0.034 ± 0.025		0.060 ± 0.011	

[a]$P < 0.05$.

was strongly associated with a poor prognosis of NBL ($P < 0.00001$; Fig. 4A, middle). Remarkably, the combination of low levels of both *NLRR3* and *Miz-1* expressions showed a significantly worse prognosis as compared with the other combination, high *NLRR3* and *Miz-1* expressions ($P = 0.0012$; Fig. 4C). Furthermore, the combination of low expression of *NLRR3* and high expression of *MYCN* showed a significantly worse prognosis than the combination of high expression of *NLRR3* and low expression of *MYCN* ($P < 0.00001$; Fig. 4B). In NBLs with low expression of *MYCN*, the expression levels of *NLRR3* could segregate the prognosis into good and intermediate groups.

The univariate Cox regression analysis shown in Table 2 was employed to examine the individual relationship of each variable to survival. The results in Table 2 showed that *NLRR3* expression, *MYCN* expression, *Miz-1* expression, age, *MYCN* amplification, stage *TrkA* expression, and origin were of prognostic importance, supporting the results of the log-rank test. Moreover, the multivariate Cox models were fitted to assess the predictive importance of NLRR3 expression for survival after controlling other prognostic factors. The results in Table 2 showed that *NLRR3* expression was significantly associated with survival after controlling *TrkA* expression ($P = 0.0212$), suggesting that *NLRR3* expression was an independent prognostic factor from *TrkA* expression (Table 2). This suggests that *NLRR3* expression is associated with survival after controlling *MYCN* expression ($P = 0.0610$), *Miz-1* expression ($P = 0.1510$), *MYCN* amplification ($P = 0.1210$), and stage ($P = 0.1040$), and also supports that *NLRR3* expression could serve as a prognostic biomarker for NBL tumors dependent on both MYCN and Miz-1 expression as well as *MYCN* amplification.

Discussion

In primary human NBLs, *MYCN* is frequently amplified and thereby one of the most important prognostic factors. In this study, we found that *NLRR3* is a direct target of MYCN but its expression is negatively regulated by MYCN in association with Miz-1. In primary NBLs, both *NLRR3* and *Miz-1* are expressed at significantly high levels in favorable NBLs and downregulated in *MYCN*-amplified aggressive tumors.

In general, favorable NBL cells show more differentiated features than unfavorable cells (30). The treatment of NBL cells with ATRA induces neuronal differentiation accompanied with growth inhibition and reduction of *MYCN* expression (33). Under such conditions, *NLRR3* is induced while *MYCN* is decreased (Figs. 1 and 2). These results suggest a functional inverse relationship between MYCN and NLRR3 in cellular differentiation and tumor development. In some NBL cell lines, siRNA-mediated knockdown of endogenous MYCN caused NLRR3 induction; conversely, ectopic expression of MYCN resulted in a decreased expression of *NLRR3*. Hence, the inverse regulatory relationship between NLRR3 and MYCN may be present as a

Published OnlineFirst September 9, 2011; DOI:10.1158/1078-0432.CCR-11-0313

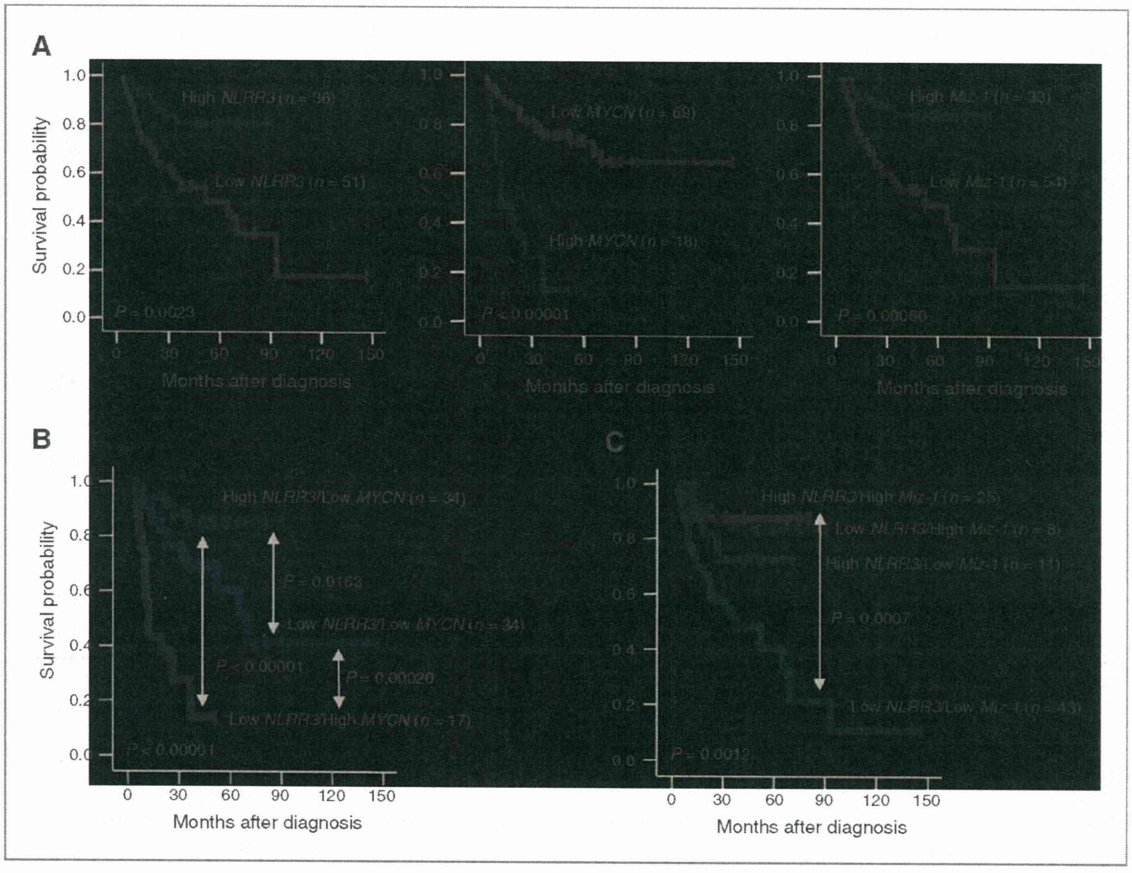

Figure 4. Real-time PCR analysis for the expression of *NLRR3*, *MYCN*, and *Miz-1* in 87 primary NBLs. Kaplan–Meier survival curves of patients with NBLs on the basis of higher or lower expression levels of *NLRR3* (A, left); *MYCN* (A, middle); *Miz-1* (A, right); *NLRR3* and *MYCN* (B); or *NLRR3* and *Miz-1* (C). In case of *NLRR3* and *MYCN* survival curve, high NLRR3/high MYCN group was excluded because this group consists of only 2 samples. Relative expression levels of *NLRR3* or *MYCN* or *Miz-1* mRNA were determined by calculating the ratio between *GAPDH* and *NLRR3* or *MYCN* or *Miz-1*.

consequence of MYCN-induced transcriptional downregulation of *NLRR3*.

MYCN protein is an important regulator of many cellular processes, including growth, proliferation, differentiation, and apoptosis (42). A part of these diverse cellular functions of MYCN may be due to the combined abilities of both activating and repressing transcription of the target genes (42). Transcriptional activation by MYCN occurs *via* dimerization with its partner protein, Max, and direct binding to specific DNA sequences named E-boxes. MYCN directly binds and stimulates the expression of approximately 4,000 of the E-box containing genes (43). Although heterodimerization of Max with MYCN is necessary to regulate gene expression, the other proteins including *Miz-1* may bind to C-terminal MYCN in addition to Max (19, 20, 44). Concurrent binding of these factors redirects the MYCN/Max dimer to noncanonical sites such as the initiator element, where this complex might prevent the efficient binding of basal transcriptional machinery or coactivators necessary for transactivation, resulting in repression of gene expression (38, 44). The dimerization with MYCN switches Miz-1 from a transcriptional activator to a repressor of the target genes, likely by preventing the interaction of Miz-1 with its own coactivator (19, 20). Several studies have shown that Miz-1 binds and activates the promoter of several genes, including $p15^{INK4b}$ and $p21^{CIP1}$, and the transactivation can be negatively regulated by its association with MYCN (16, 17, 29). Regarding the reduction of NLRR3 expression observed in this study, Miz-1 seems to be a key molecule forming a transcription factor complex with MYCN. Because Miz-1 itself acts as an activator of *NLRR3* promoter, *NLRR3* expression may be switched on and off through Miz-1 in the absence and presence of MYCN, respectively. Although the expression levels of Miz-1 in unfavorable NBLs are relatively low, its amount still may be enough to act with MYCN to inhibit transactivation of *NLRR3* in NBLs.

Published OnlineFirst September 9, 2011; DOI:10.1158/1078-0432.CCR-11-0313

Table 2. Multiple Cox regression model using NLRR3 expression and dichotomous factors of MYCN expression, Miz-1 expression, age, MYCN amplification, stage, TrkA expression, and origin ($n = 87$)

Model	Factor	*P*	HR (95% CI)
Univariate analysis			
A	*NLRR3* mRNA expression (high vs. low)	0.0041[a]	0.291 (0.125–0.678)
B	*MYCN mRNA* expression (high vs. low)	<0.0001[a]	5.050 (2.450–10.40)
C	*Miz-1* mRNA expression (high vs. low)	0.0021[a]	0.212 (0.080–0.561)
D	Age (≥1 vs. <1 y)	0.0161[a]	0.309 (0.119–0.803)
E	*MYCN* amplification (single copy vs. amplified)	<0.0001[a]	4.628 (2.281–9.387)
F	Stage (1,2,4s vs. 3,4)	0.0010[a]	12.66 (3.023–53.09)
G	*TrkA* expression (high vs. low)	0.0070[a]	7.180 (1.714–30.07)
H	Origin (adrenal gland vs. others)	0.0480[a]	2.125 (1.005–4.491)
Multivariate analysis			
A	*NLRR3* mRNA expression (high vs. low)	0.061	0.424 (0.172–1.041)
	MYCN mRNA expression (high vs. low)	0.0011[a]	3.707 (1.735–7.921)
B	*NLRR3* mRNA expression (high vs. low)	0.151	0.503 (0.198–1.283)
	Miz-1 mRNA expression (high vs. low)	0.0301[a]	0.304 (0.104–0.893)
C	*NLRR3* mRNA expression (high vs. low)	0.0150[a]	0.347 (0.148–0.814)
	Age (≥1 vs. <1 y)	0.053	0.384 (0.146–1.013)
D	*NLRR3* mRNA expression (high vs. low)	0.121	0.545 (0.253–1.173)
	MYCN amplification (single copy vs. amplified)	0.0001[a]	3.940 (1.893–8.203)
E	*NLRR3* mRNA expression (high vs. low)	0.104	0.493 (0.210–1.156)
	Stage (1, 2, 4s vs. 3, 4)	0.0020[a]	10.108 (2.359–43.309)
F	*NLRR3* mRNA expression (high vs. low)	0.0212[a]	0.361 (0.152–0.863)
	TrkA expression (high vs. low)	0.0163[a]	5.892 (1.395–24.901)
G	*NLRR3* mRNA expression (high vs. low)	0.0070[a]	0.308 (0.132–0.720)
	Origin (adrenal gland vs. others)	0.084	1.937 (0.914–4.104)

NOTE: All variables with 2 categories. HR shows the relative risk of death of first category relative to the second.
[a]$P < 0.05$.

Inhibition of cellular differentiation is one of the well-known biological functions of MYCN. Because differentiated NBL cells have a high expression of NLRR3 instead of MYCN, the reduced expression of NLRR3 in undifferentiated, unfavorable NBL cells may propose an important component of the mechanism by which MYCN functions against cell differentiation. As ectopic expression of NLRR3 induced morphologic changes indicative of neuronal differentiation accompanying with neurite outgrowth (data not shown), the downregulation of NLRR3 by MYCN might contribute to the well-documented stimulation of cell proliferation by MYCN. Although there are MYCN target genes that are potentially involved in cell-cycle progression, including *α-prothymosin, ornithine decarboxylase, MCM7, ID2, MDM2,* and *NLRR1* (27, 36, 45–47), suppression of NLRR3 might have an additive effect on NBL cell proliferation. Our log-rank test showed that expression of NLRR3 is well associated with a favorable prognosis, suggesting its involvement in NBL differentiation. Of more interest, NLRR3 and NLRR1 seem to function oppositely in NBL. Thus, the expression of NLRR3 is a new prognostic indicator of NBL and may be involved in regulating the biology of the tumor.

Collectively, our present findings suggest that the repression of NLRR3 mediated by MYCN requires an association with Miz-1 and also contributes to the favorable outcome of NBLs. The expression pattern of NLRR3, Miz-1, and MYCN might play an important role in defining the clinical behavior of NBLs. Because NLRR3 is an orphan receptor, the future discovery of its ligand(s) may unveil the molecular mechanism of tumorigenesis, differentiation, and proliferation of NBL. Further investigation is necessary to clarify whether NLRR3 is an important primary cue for developing novel diagnostic and therapeutic strategies against high-risk NBLs.

Disclosure of Potential Conflicts of interest

No potential conflicts of interest were disclosed.

Acknowledgments

The authors thank Drs. Y. Nakamura and E. Isogai (Chiba Cancer Center Research Institute, Chiba, Japan) for their outstanding technical assistance, and Dr. Hiroki Nagase (Chiba Cancer Center Research Institute, Chiba, Japan) and Ms. Paula D. Jones (Roswell Park Cancer Institute, Buffalo, NY) for critical reading of the article.

Published OnlineFirst September 9, 2011; DOI:10.1158/1078-0432.CCR-11-0313

Grant Support

This work was supported in part by a grant-in-aid from the Ministry of Health, Labour and Welfare for Third Term Comprehensive Control Research for Cancer (A. Nakagawara), a grant-in-aid for Scientific Research on Priority Areas from the Ministry of Education, Culture, Sports, Science and Technology, Japan (A. Nakagawara), and a grant-in-aid for Scientific Research from the Japanese Society for the Promotion of Science (A. Takatori and A. Nakagawara).

The costs of publication of this article were defrayed in part by the payment of page charges. This article must therefore be hereby marked *advertisement* in accordance with 18 U.S.C. Section 1734 solely to indicate this fact.

Received February 3, 2011; revised August 3, 2011; accepted August 9, 2011; published OnlineFirst September 9, 2011.

References

1. Westemann F, Schwab M. Genetic parameters of neuroblastomas. Cancer Lett 2002;184:127–47.
2. Brodeur GM, Nakagawara A. Molecular basis of clinical heterogeneity in neuroblastoma. Am J Pediatr Hematol Oncol 1992;14:111–6.
3. Nakagawara A, Arima M, Azar CG, Scavarda NJ, Brodeur GM. Inverse relationship between trk expression and N-myc amplification in human neuroblastomas. Cancer Res 1992;52:1364–68.
4. Nakagawara A, Arima-Nakagwara M, Scavarda NJ, Azar CG, Cantor AB, Brodeur GM. Association between high levels of expression of the TRK gene and favorable outcome in human neuroblastoma. New Engl J Med 1993;328:847–54.
5. Nakagawara A, Azar CG, Scavarda NJ, Brodeur GM. Expression and function of TRK-B and BDNF in human neuroblastomas. Mol Cell Biol 1994;14:759–67.
6. Nakagawara A, Arima-Nakagawara M, Azar CG, Scavarda NJ, Brodeur GM. Clinical significance of expression of neurotrophic factors and their receptors in neuroblastoma. Prog Clin Biol Res 1994;385:155–61.
7. Seeger RC, Brodeur GM, Sather H, Dalton A, Siegel SE, Wong KY, et al. Associations of multiple copies of the N-myc oncogene with rapid progression of neuroblastomas. New Engl J Med 1985;313:1111–6.
8. Kohl NE, Gee CE, Alt FW. Activated expression of the N-myc gene in human neuroblastomas and related tumors. Science 1984;226:1335–7.
9. Nisen PD, Waber PG, Rich MA, Pierce S, Garvin JR, Gilbert F, et al. N-myc oncogene RNA expression in neuroblastoma. J Natl Cancer Inst 1988;80:1633–7.
10. Slavc I, Ellenbogen R, Jung WH, Vawter GF, Kretschmar C, Grier H, et al. Myc gene amplification and expression in primary human neuroblastoma. Cancer Res 1990;50:1459–63.
11. Seeger RC, Wada R, Brodeur GM, Moss TJ, Bjork RL, Sousa L, et al. Expression of N-myc by neuroblastomas with one or multiple copies of the oncogene. Prog Clin Biol Res 1988;271:41–9.
12. Schwab M, Ellison J, Busch M, Rosenau W, Varmus HE, Bishop JM. Enhanced expression of the human gene N-myc consequent to amplification of DNA may contribute to malignant progression of neuroblastoma. Proc Natl Acad Sci U S A 1984;81:4940–4.
13. Cohn SL, Tweddle DA. MYCN amplification remains prognostically strong 20 years after its "clinical debut". Eur J Cancer 2004;40:2639–42.
14. Strieder V, Lutz W. Regulation of N-myc expression in development and diseases. Cancer Lett 2002;180:107–19.
15. Kouzarides T, Ziff E. The role of the leucine zipper in the fos-jun interaction. Nature 1988;336:646–51.
16. Landschulz WH, Johnson PF, Mcknight SL. The leucine zipper: a hypothetical structure common to a new class of DNA binding proteins. Science 1988;240:1759–64.
17. Alex R, Sozeri O, Meyer S, Dildrop R. Determination of the DNA sequence recognized by the bHLH-zip domain of the N-Myc protein. Nucleic Acids Res 1992;20:2257–63.
18. Blackwood EM, Kretzner L, Eisenman RN. Myc and Max function as a nucleoprotein complex. Curr Opin Genet Dev 1992;2:227–35.
19. Staller P, Peukert K, Kiermaier A, Seoane J, Lukas J, Karsunky H, et al. Repression of p15INK4b expression by Myc through association with Miz-1. Nature Cell Biol 2001;3:392–9.
20. Wu S, Cetinkaya C, Munoz-Alonso MJ, Von der Lehr N, Bahram F, Beuger V, et al. Myc represses differentiation-induced p21CIP1 expression via Miz-1-dependent interaction with the p21 core promoter. Oncogene 2003;22:351–60.
21. Zhang J, Li F, Liu X, Shen L, Liu J, Su J, et al. The repression of human differentiated-related gene NDRG2 expression by Myc via Miz-1 dependent interaction with the NDRG2 core promoter. J Biol Chem 2006;281:39159–68.
22. Koppen A, Ait-Aissa R, Hopman S, Koster J, Haneveld F, Versteeg R, et al. Dickkopf-1 is down-regulated by MYCN and inhibits neuroblastoma cell proliferation. Cancer Lett 2007;256:218–28.
23. Hamano S, Ohira M, Isogai E, Nakada K, Nakagawara A. Identification of novel human neuronal leucine-rich repeat (hNLRR) family genes and inverse association of expression of Nbla10449/hNLRR-1 and Nbla10677/hNLRR-3 with the prognosis of primary neuroblastomas. Int J Oncol 2004;24:1457–66.
24. Ohira M, Morohashi A, Inuzuka H, Shishikura T, Kawamoto T, Kageyama H, et al. Expression profiling and characterization of 4200 genes cloned from primary neuroblastomas: identification of 305 genes differentially expressed between favorable and unfavorable subsets. Oncogene 2003;22:5525–36.
25. Hayata T, Uochi T, Asashima M. Molecular cloning of XNLRR-1, a Xenopus homolog of mouse neuronal leucine-rich repeat protein expressed in the developing Xenopus nervous system. Gene 1998;221:159–66.
26. Fukamachi K, Matsuoka Y, Ohno H, Hamaguchi T, Tsuda H. Neuronal leucine-rich repeat protein-3 amplifies MAPK activation by epidermal growth factor through a carboxyl-terminal region containing endocytosis motifs. J Biol Chem 2002;277:43549–52.
27. Hossain MS, Ozaki T, Wang H, Nakagawa A, Takenobu H, Ohira M, et al. N-MYC promotes cell proliferation through a direct transactivation of neuronal leucine-rich repeat protein-1 (NLRR1) gene in neuroblastoma. Oncogene 2008;27:6075–82.
28. Ishii N, Wanaka A, Tohyama M. Increased expression of NLRR-3 mRNA after cortical brain injury in mouse. Molecular Brain Research 1996;40:148–52.
29. Brodeur GM, Pritchard J, Berthold F, Carlsen NL, Castel V, Castelberry RP, et al. Revisions of the international criteria for neuroblastoma. Diagnosis, staging, and response to treatment. J Clin Oncol 1993;11:1466–77.
30. Matsumura T, Iehara T, Sawada T, Tsuchida Y. Prospective study for establishing the optimal therapy of infantile neuroblastoma in Japan. Med Pediatr Oncol 1998;31:210.
31. Kaneko M, Nishihira H, Mugishima H, Ohnuma N, Nakada K, Kawa K, et al. Stratification of treatment of stage 4 neuroblastoma patients based on N-myc amplification status. Study Group of Japan for Treatment of Advanced Neuroblastoma, Tokyo, Japan. Med Pediatr Oncol 1998;31:1–7.
32. Melino G, Thiele CJ, Knight RA, Piacentini M. Retinoids and the control of growth/death decisions in human neuroblastoma cell lines. J Neurooncol 1997;31:65–83.
33. Thiele CJ, Reynolds CP, Israel MA. Decreased expression of N-myc precedes retinoic acid-induced morphological differentiation of human neuroblastoma. Nature 1985;313:404–6.
34. Niizuma H, Nakamura Y, Ozaki T, Nakanishi H, Ohira M, Isogai E, et al. Bcl-2 is a key regulator for the retinoic acid-induced apoptopic cell death in neuroblastoma. Oncogene 2006;25:5046–55.
35. Bjelfman C, Meyerson G, Cartwright CA, Mellstrom K, Hammerling U, Pahlman S. Early activation of endogenous pp60src kinase activity during neuronal differentiation of cultured human neuroblastoma cells. Mol Cell Biol 1990;10:361–70.

Published OnlineFirst September 9, 2011; DOI:10.1158/1078-0432.CCR-11-0313

36. Lutz W, Stohr M, Schurmann J, Wenzel A, Lohr A,Schwab M. Conditional expression of N-myc in human neuroblastoma cells increases expression of α-prothymosin and ornithine decarboxylase and accelerates progression into S-phase after mitogenic stimulation of quiescent cells. Oncogene 1996;13:803–12.
37. Chen L, Peng Z, Bateman E. In vivo interactions of the Acanthamoeba TBP gene promoter. Nucleic acids Res 2004;32: 1251–60.
38. Peukert K, Staller P, Schneider A, Carmichael G, Hanel F,Eilers M. An alternative pathway for gene regulation by Myc. EMBO J 1997;16: 5672–86.
39. Shimada H, Ambros IM, Dehner LP, Hata J, Joshi VV, Roald B, et al. The International Neuroblastoma Pathology Classification (the Shimada System). Cancer 1999;86: 364–72.
40. Ikegaki N, Gotoh T, Kung B, Riceberg JS, Kim DY, Zhao H, et al. De novo identification of MIZ-1 (ZBTB17) encoding a MYC-interacting zinc-finger protein as a new favorable neuroblastoma gene. Clin Cancer Res 2007;13:6001–9.
41. Tang XX, Zhou H, Kung B, Kim DY, Hicks SL, Cohn SL, et al. The MYCN enigma: significance of MYCN expression in neuroblastoma. Cancer Res 2006;66:2826–33.
42. Pelengaris S, Khan M, Evan G. c-MYC: more than just a matter of life and death. Nat Rev Cancer 2002;2:764–76.
43. Levens DL. Reconstructing MYC. Genes dev 2003;17:1071–7.
44. Wanzel M, Herold S, Eilers M. Transcriptional repression by Myc. Trends Cell Biol 2003;13:146–50.
45. Shohet JM, Hicks MJ, Plon SE, Burlingame SM, Stuart S, Chen SY, et al. Minichromosome maintenance protein MCM7 is a direct target of the MYCN transcription factor in neuroblastoma. Cancer Res 2002;62:1123–8.
46. Iasorella A, Noseda M, Beyna M, Yokota Y, Iavarone A. Id2 is a retinoblastoma protein target and mediates signaling by Myc oncoproteins. Nature 2000;407:592–8.
47. Slack A, Chen Z, Tonelli R, Pule M, Hunt L, Pession A, et al. The p53 regulatory gene MDM2 is a direct transcriptional target of MYCN in neuroblastoma. Proc Natl Acad Sci U S A 2005;102:731–6.